REMOVAL OF METHYL ORANGE FROM AQUEOUS SOLUTIONS USING TiO_2 PHOTOCATALYST, POLYANILINE ADSORBENT AND THE COMBINED TiO_2 – POLYANILINE

By

KARAM HAITHAM WAZIR

Thesis submitted in fulfillment of the requirements for the degree of Doctor of Philosophy

March 2015

AKNOWLEDGEMENT

IN THE NAME OF ALLAH THE MOST GRACIOUS AND MOST MERCIFUL

Thanks to Allah S.W.T for giving me the opportunity to do this thesis successfully. I would take opportunity to express my profound gratitude and deep regards to my supervisor Professor Dr. Mohd Asri Nawi, for his help, professionalism, valuable guidance and constant encouragement throughout the course of this work.

I would like to acknowledge Postgraduate Research Grant (PGRS: 1001/PKIMIA/845021) and FRGS Grant: 203/PKIMIA/6711228) for providing the financial supports to this research. I would also like to express a sense of gratitude to my colleagues, I am grateful for their cooperation during the period of my research. Not forgetting all the respective lecturers and staffs of school of Chemical Sciences, School of Biological Science, School of Physics, and Institute of Postgraduate studies (IPS) for the cooperation, and also those had contributed either directly or indirectly to accomplish this research.

My endless appreciation goes to my husband, Hamza Khalil Khoja. I am truly appreciative of all that he has done for me over the years. I could not have reached my goals without his help and support at all times. The same goes to my lovely children, Nour Hamza, Anas Hamza and Aws Hamza.

Last but not least, I would like to extend my gratitude to my parents, brothers, sisters and friends for their constant encouragement without which this accomplishment would not be possible. Thank you

TABLE OF CONTENTS

LIST OF TABLES

LIST OF FIGURES

LIST OF ABBREVIATIONS

AOPs	Advanced oxidation processes
WW	Wastewater treatment
$OH^{\cdot}$	hydroxyl radicals
$O_2^{\cdot -}$	superoxide radical
$HO_2^{\cdot}$	hydroperoxyl radical
Eg	Band-gap energy
eV	Electronvolt
TiO_2	Titanium dioxide
DSSC	dye sensitized solar cell
e^-	Negative electron
h^+	Positive hole
R	recalcitrant organic compound
UV	Ultraiolet
HOMO	highest occupied molecular orbital
LUMO	lowest unoccupied molecular orbital
EPD	electrophoretic deposition
MO	Methyl orange
PANI	Polyaniline
ES	Emeraldine salt
ECP	Electrochemical process
HA	Humic acid

MWNT	multiwall carbon nanotube
PVP	Polyvinylpyrrolidone
APS	Ammonium peroxydisulfate
ENR-50	Epoxidized natural rubber
PVC	Polyvinyl cloride
W	Watt
H	hour
µm	Micrometer
EB	Emeraldine base
Nm	nanometer
BET	Brunauer-Emmett-Teller
L	Liter
µL	Microliter
Min	minute
M	Molarity
Pzc	point of zero charge
RR4	Reactive Red 4

LIST OF PUBLICATIONS AND CONFERENCES

International journal

Karam, H., M.A.M Nawi and S. Razak, 2014. Kinetics and Isotherm Studies of Methyl Orange Adsorption onto a Highly Reusable Immobilized Polyaniline on Glass Plate. *Arabian Journal of Chemistry*, doi:10.1016/j.arabjc.2014.10.010.

S. Razak, M.A.M Nawi and **Karam, H.,** 2014. Fabrication, Characterization and Application of a Reusable Immobilized TiO_2-PANI Photocatalyst Plate for the Removal of Reactive Red 4 dye. *Applied Surface Science Journal*, 319, 90-98.

Proceedings

Karam, H., and M.A.M Nawi, (2012). "Parameters affecting the photocatalytic Decolourization of Methyl Orange (MO) Using Immobilized Nanoparticles of TiO2". International Conference on Environment (ICENV), Penang, Malaysia 11th - 13th December 2012.

Karam, H., and M.A.M Nawi, (2013). **"**Parameters affecting the photocatalytic regeneration of immobilized PANI adsorbent by P-25 TiO_2 for the removal of methyl orange dye'**.** International Conference on Engineering and Applied Science (HKICEAS), Hong Kong, 19th-21st December (2013).

Conferences and Seminar attended:

Karam, H., and M.A.M Nawi, "Adsorption of Methyl Orange by Immobilized Polyaniline on Glass Plate", The 24th Regional Symposium of Malaysian Analytical Sciences (SKAM), One Hotel Helang, Langkawi, Malaysia 21st - 23rd November 2011

Karam, H., and M.A.M Nawi, (2012). "Adsorption of Methyl Orange by Suspended and Immobilized Polyaniline on Glass Plate", School of chemical Sciences Seminar (2012), USM, Penang.

Karam, H., and M.A.M Nawi, (2012). "Parameters affecting the photocatalytic Decolourization of Methyl Orange (MO) Using Immobilized Nanoparticles of TiO_2". International Conference on Environment (ICENV), Penang, Malaysia 11th-13th December 2012.

Karam, H., and M.A.M Nawi, (2013). **"**Parameters affecting the photocatalytic regeneration of immobilized PANI adsorbent by P-25 TiO_2 for the removal of methyl orange dye'**.** International Conference on Engineering and Applied Science (HKICEAS), Hong Kong, 19^{th}-21^{st} December (2013).

PENYINGKIRAN METIL JINGGA DARIPADA LARUTAN AKUEUS MENGGUNAKAN FOTOMANGKIN TiO_2 TERIMOBILISASI, PENJERAP POLIANILINA DAN GABUNGAN TiO_2 – POLIANILINA

ABSTRAK

Penguraian fotopemangkinan metil jingga (MO) dengan fotomangkin P-25 TiO_2 terimobilisasi pada plat kaca melalui kaedah salutan-celup dijalankan dalam bahagian pertama kajian ini. Parameter optimum yang diperoleh bagi penguraian fotopemangkinan larutan MO ditemui pada pH 2, muatan mangkin 1.88 mg cm^{-2} dan kadar pengudaraan 40 mL min^{-1}. Pemalar kadar (k) adalah 0.045 min^{-1} tetapi meningkat kepada 0.062 min^{-1} dalam kehadiran 0.017 mg L^{-1} H_2O_2. Plat fotomangkin terimobilisasi boleh digunakan bagi banyak kitaran aplikasi yang berulang. Namun demikian, nilai k berkurangan daripada 0.062 min^{-1} dengan 33.2 % tinggalan MO bagi aplikasi pertama kepada 0.049 min^{-1} dengan 43.6 % tinggalan MO pada kitaran aplikasi ke-10. Kaedah salutan-celup yang mudah juga digunakan bagi penghasilan polianilina terimobilisasi (PANI) pada plat kaca dengan menggunakan polivinilpirolidon (PVP) sebagai perekat. Pada bahagian kedua kajian ini, PANI disalut pada plat kaca (PANI/kaca) dan PANI berbentuk serbuk dibandingkan dalam penyingkiran MO daripada larutan akueus. pH optimum bagi penyingkiran MO adalah 7, muatan PANI optimum adalah 0.63 mg cm^{-2} dengan ketebalan 18.20 μm. Penjerapan maksimum q_{max} bagi PANI/kaca dan serbuk PANI masing-masing adalah 91 dan 147 mg g^{-1}. Di samping itu, model tertib pseudo-kedua adalah model kinetik yang sesuai bagi kedua-dua sistem, yang membawa erti kadar penghad mungkin bersifat pengkimiaserapan. Nilai tenaga bebas dan entalpi menunjukkan bahawa proses penjerapan adalah spontan dan eksotermik. Berbeza

dengan serbuk PANI, PANI/kaca menghasilkan entalpi negatif. Kitaran semula PANI terimobilisasi yang telah terguna dijalankan melalui proses penjanaan semula fotopemangkinan dengan menggunakan buburan P-25TiO_2 sebagai fotomangkin. Penyahjerapan MO daripada PANI terimobilisasi dilakukan dengan menggunakan larutan 25 mL 0.005 M H_2SO_4 pada peringkat pertama, dan larutan 25 mL 0.5 M H_2SO_4 pada peringkat kedua proses penjanaan semula. Keadaan optimum pemfotorosotaan MO yang ternyah-jerap oleh 30 mg serbuk TiO_2 adalah pH 2, kadar pengudaraan 80 mL min^{-1} dan 0.028 mg L^{-1} H_2O_2. Penjerap PANI terimobilisasi diguna semula bagi sekurang-kurangnya 20 kali penyingkiran daripada larutan 20 mL 60 mg L^{-1} MO, dan proses penjanaan semula dilakukan selepas setiap lima kitaran plat PANI/ kaca yang sama. Kajian akhir melibatkan sistem dwilapisan TiO_2/PANI. Muatan optimum sublapisan PANI dan lapisan atas TiO_2 adalah 0.63 mg cm^{-2}. Pada keadaan ini, kedua-dua proses fotopemangkinan dan penjerapan berlaku secara serentak. Nilai R^2 adalah 0.968 dan 0.929 masing-masing bagi model isoterma Freundlich dan Langmuir. Kedua-dua $q_{e.cal}$ dan $q_{e.exp}$ sama di antara satu sama lain, dan nilai R^2 pula adalah lebih tinggi daripada 0.99 apabila persamaam tertib pseudo-kedua diaplikasikan. Justeru, dapat dicadangkan bahawa, penjerapan MO melalui sistem dwilapisan TiO_2/PANI mematuhi isoterma Freundlich dan mengikuti persamaan kinetik tertib kedua. Peratusan baki MO selepas proses fotopemangkinan oleh TiO_2/PANI adalah 27.4 % manakala bakinya bernilai 88.2 % selepas proses penjerapan pada kitaran ke-10. Berdasarkan peratus baki MO untuk 10 aplikasi kitaran, sistem dwilapisan TiO_2/PANI merupakan yang terbaik jika dibandingkan dengan sistem lapisan tunggal PANI/kaca dan TiO_2/kaca.

REMOVAL OF METHYL ORANGE FROM AQUEOUS SOLUTIONS USING IMMOBILIZED TiO_2 PHOTOCATALYST, POLYANILINE ADSORBENT AND THE COMBINED TiO_2 – POLYANILINE

ABSTRACT

The photocatalytic degradation of MO by P-25TiO_2 photocatalyst immobilized on glass plates via a dip coating method has been carried out in this first part of the study. The optimum parameters obtained for the photocatalytic degradation of MO solution were found to be pH 2, catalyst loading of 1.88 mg cm^{-2} and aeration rate of 40 mL min^{-1}. The observed rate constant (k) was 0.045 min^{-1} but increased to 0.062 min^{-1} in the presence of 0.017 mg L^{-1} H_2O_2. The immobilized photocatalyst plate can be used for many repeated cycles of applications. However, the k values decreased from 0.062 min^{-1} to 0.049 min^{-1} while percent MO remained increased from 33.2 % for the first application to 43.6 % at the 10th cycle of application. The simple dip coating method was also used for immobilizing polyanailine (PANI) onto glass plates using polyvinylpyrrolidone (PVP) as an adhesive. In this second part of the study, PANI coated onto glass plates (PANI/glass) and their powder forms were compared in the removal of MO dye from aqueous solutions. It was found that the optimum pH for the removal of MO was 7 and the optimum PANI loading was 0.63 mg cm^{-2} corresponding to 18.20 μm in thickness. The maximum adsorption q_{max} for PANI/glass and PANI powder was 91 and 147 mg g^{-1} respectively. In addition, the pseudo-second order model was the best fitted kinetic model for both systems, suggesting that the rate-limiting step may be chemisorption. The obtained negative values of free energy and enthalpy indicated the adsorption process was spontaneous and exothermic. In contrast to powder PANI, PANI/glass yielded negative entropy.

The recycling of the used immobilized PANI was carried out via a photocatalytic regeneration process using P-25TiO_2 slurry as the photocatalyst. The desorption of MO from the immobilized PANI was carried out using a 25 mL 0.005 M H_2SO_4 solution in the first stage and a 25 mL 0.5 M H_2SO_4 solution in the second stage of the regeneration process. The optimum conditions for the photodegradation of the desorbed MO by 30 mg TiO_2 powder was pH 2, aeration rate of 80 mL min^{-1} and 0.028 mg L^{-1} H_2O_2. The immobilized PANI adsorbent was reused for at least 20 times for the removal of 20 mL of 60 mg L^{-1} MO solution whereby a regeneration process was done after every five runs of the same PANI/glass plate. The final study involved the TiO_2/PANI bilayer system. The optimum loading of the PANI sub layer and the TiO_2 top layer was 0.63 mg cm^{-2}. Under this condition, both photocatalysis and adsorption processes occurred simultaneously. The R^2 values were 0.968 and 0.929 for the Freundlich and the Langmuir isotherm models. The $q_{e.cal}$ and $q_{e.exp}$ was in agreement with each other and the R^2 was higher than 0.99 when the pseudo-second order equation was applied. Therefore, it could be suggested that, the adsorption of MO by the TiO_2/PANI bilayer system obeyed Freundlich isotherm and followed second order kinetic equation. The percent remained of MO after the photocatalytic process by TiO_2/PANI was 27.4 % while it was 88.2 % after the 10th run of the adsorption process. Based on the percent remained of MO for 10 cycles of applications, the TiO_2/PANI bilayer was found the better system in comparison with single layer systems of PANI/glass and TiO_2/glass.

CHAPTER ONE

INTRODUCTION

1.1 General

Synthetic dyes have been commonly used in the textile, food, paper making leather and cosmetic industries (Parshetti et al., 2010). It is estimated that 10-15 % of the dye is lost during the dyeing process and released as effluent (Lachheb et al., 2002 and Guettai & Amar, 2005). Those coloured effluents are a considerable major environmental problem. The coloured effluents influence the natural aspect of rivers and have a negative impact upon aquatic life. They are viewed as a source of non-aesthetic pollution as the small concentration of dyes (below 1 ppm) is clearly visible and would reduce the action of photosynthesis (Konstantinou & albanis, 2004; Karkmaz et al., 2004 and Chen et al., 2008). Above all, many synthetic azo dyes show exhibit toxic, carcinogenic and genotoxic effects on human and aquatic life forms (Damodar et al., 2007). Thus, the wastewater must be treated before it can be released into the natural environment. For this purpose, several physical techniques have been developed such as adsorption, reverse osmosis, ion exchange on synthetic adsorbent resins, etc. Generally these techniques can be quite efficient but they are non-destructive by nature where the pollutants are actually being transferred from water to another phase, causing a secondary pollution (Konstantinou & Albanis, 2004). Biological decolourization is an inefficient treatment process as most of azo dyes are resistant to aerobic bio-degradation (Zhu et al., 2012). Moreover, carcinogenic aromatic amines might be generated from anaerobic bio-degradation of azo dyes (Wong & Yuen, 1996). From the economical view point, chemical methods are not practical as they require high dosage of chemicals and produce large amount of sludge (Baban et al., 2003).

1.2 Advance Oxidation Process (AOPs)

In order to produce water with acceptable levels of persistent pollutants such as pesticides, solvents and phenols, a further treatment stage is needed. Application of advanced oxidation processes (AOPs) are recommended when wastewater components have a high chemical stability and/or low biodegradability (Poyatos et al., 2010). Figure 1.1 shows various applications of AOPs in the wastewater treatment process.

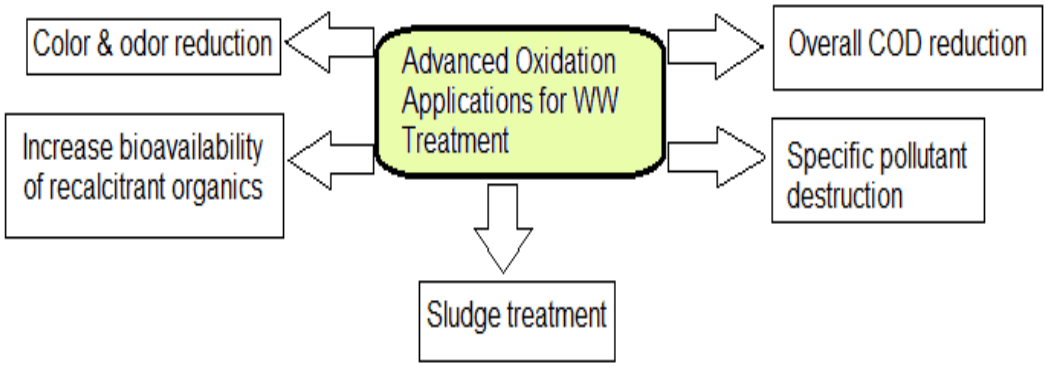

Figure1.1: Application of AOPs for WW treatment (Bergendahl & O'shaughnessy 2004).

A chemical wastewater treatment using AOPs can complete the mineralization of pollutants to CO_2, water and inorganic compounds as shown in equation 1.1 or at least their transformation into more innocuous products (Lachheb et al., 2002; Karkmaz et al., 2004 and Poyatos et al., 2010).

$$AOP_s \longrightarrow OH^{\bullet} \xrightarrow{\text{pollutant}} CO_2 + H_2O + \text{inorganic ions} \qquad (1.1)$$

Advanced oxidation processes (AOPs) represent new methods for wastewater treatment. They can be implemented at near ambient temperature and pressure. These treatment processes operate by generating powerful oxidizing species such as hydroxyl radicals ($OH^{\cdot}$), superoxide radical ($O_2^{\cdot -}$), hydroperoxyl radical ($HO_2^{\cdot}$), and

alkoxyl radical (Wang & XU, 2012) which in turn can oxidize the organic pollutants into CO_2 and H_2O or other more innocuous products.

Among these various radicals, the hydroxyl radical is thought to play a central role in the AOPs applications for wastewater treatment. This hydroxyl radical reacts typically million times faster than ozone and hydrogen peroxide. The oxidation power of various oxidizing agents are listed in Table 1.1 (Vogelpohl & Kim, 2004). In addition, hydroxyl radicals can be generated from different systems which can include photochemical degradation processes (UV/O_3, UV/H_2O_2), photocatalysis (TiO_2/UV, photo-Fenton reactive), and chemical oxidation processes (O_3, O_3/H_2O_2, H_2O_2/Fe^{2+}), electron beam irradiation and sonolysis (Xu & Jin, 2012; (Vogelpohl & Kim, 2004 and Poyatos et al., 2010).

Table 1.1: Oxidation species and their oxidation power (Vogelpohl & Kim, 2004)

Oxidation species	Oxidation power
Hydroxyl radical	2.05
Atomic oxygen	1.78
Ozone	1.52
Hydrogen peroxide	1.31
Permanganate	1.24
Chlorine	1.00

These various systems were shown to be effective in degrading and removing specific pollutants which were otherwise extremely difficult to be eliminated with conventional processes since many of these compounds are not recalcitrant pollutants. Therefore, AOPs can be regarded as a technologically efficient tool for the treatment of water especially for persistent pollutants.

1.3 Heterogeneous Photocatalysis

Among different reagent systems used by AOPs, heterogeneous photocatalysis appears to be more efficient and popular because of several reasons. The main advantages of heterogeneous photocatalysis are as follows (Poyatos et al., 2010):

- Semiconductors for photocatalysis applications are available and relatively inexpensive.
- Most of the photocatalysts, particularly TiO_2 (anatase) are chemically, biologically stable and reusable.
- Oxidative heterogeneous photocatalysis processes are able to mineralize wide range of persistent pollutants.
- Final products or by-products such as CO_2 and H_2O or other mineralized acids are eco-friendly.
- Photocatalyst can be stimulated by solar light or low energy light sources.
- Oxidation and reduction can occur simultaneously in the heterogeneous photocatalysis.

The definition of heterogeneous photocatalytic reactions is still vague due to the inclusion of a large variety of reactions: mild or total oxidations, dehydrogenation, hydrogen transfer and deuterium-alkane isotopic exchange, metal deposition, water detoxification, gaseous pollutant removal, etc. (Herrmann, 1999 and Devilliers, 2006). In addition, heterogeneous photocatalysis can be carried out in various media: gas phase, pure organic liquid phases or aqueous solutions (Sobczyński & Dobosz, 2001). In fact, it can only occur in the presence of three basic components: an emitted photon, a catalyst surface (a semiconductor material)

and oxidizing agent (Teh & Mohamed, 2011). Heterogeneous photocatalysis are usually involved through electronic excitation of a semiconductor caused by light absorption that drastically alters its ability to gain or to lose electron to generate electron-hole pairs that produce hydroxyl radicals and superoxide anions. These radicals and anions degrade pollutants into harmless by- products which subsequently degrade pollutants into harmless by- products. This degradation process can be carried out under ambient conditions, and perhaps lead to complete mineralization of organic carbon into CO_2, H_2O and minerals acids (Zain, 2012). Heterogeneous photocatalytic reactions occurred either in a slurry-type reactor where the catalyst particles are suspended in the contaminated water or in an immobilized-type reactor where the catalyst particles are immobilized onto the surface of various inert substrates of various types and configurations (Ibhadon & Fitzpatrick, 2013).

A semiconductor is defined as a material with electrical resistivity between that of an insulator and a conductor. The band electronic structure of a semiconductor consists of the highest occupied energy band (the valence band) and the lowest empty band (the conduction band), the distance between them is called a forbidden band or a band gap, Eg. This band gap determines the electronic properties of the solid, e.g. electric conductivity and the colour of the semiconductors because they absorb light having energy equal to or higher than the band gap energy (Devilliers, 2006).

The principle of the photocatalyic oxidation process has been reviewed extensively. When energy used is bigger than the band gap energy of the photocatalyst, valence band electrons on the surface of the catalyst may absorb the light energy to transit to the conduction band. The valence band produces holes possessing oxidizability (Meng & Juan, 2008). These electrons and holes can move

to the surface of the catalyst under light energy, and can react with other substances (oxidize or reduce). Photo efficiency can be reduced when the electron-hole recombination occurs, and the energy dissipated into heat (Herrmann, 1999).

Many semiconductors which have different band gap energies such as TiO_2, CdS, FeO_3, SnO_2, and WO_3 etc., have been used in heterogeneous photocatalysis Table 1.2 (Sobczyński & Dobosz, 2001). In general, wide-band gap semiconductors, such as TiO_2 prove to be a better photocatalyst than the low-band gap materials such as CdS due to the higher free energy of the photogenerated charge carriers of the former and the inherently low chemical and photochemical stability of the latter.

Table 1.2: Energy band gaps of various semiconductors (Sobczyński & Dobosz, 2001)

Semiconductor	E_g (eV)
Si	1.1
Fe_2O_3	2.3
CdS	2.5
WO_3	2.8
TiO_2 (rutile)	3.0
TiO_2 (anatase)	3.2
ZnO	3.2
SnO_2	3.5

1.4 Adsorption-desorption process

Adsorption–desorption reactions are important processes that can affect the transport of contaminants in the environment (Bhaumik et al., 2012). Desorption is a phenomenon whereby a substance is released from or through a surface.

The process is the opposite of sorption (that is, either adsorption or absorption). This occurs in a system being in the state of sorption equilibrium between bulk phase (fluid, i.e. gas or liquid solution) and an adsorbing surface (solid or boundary separating two fluids). When the concentration (or pressure) of a substance in the bulk phase is lowered, some of the desorbed substance changes to the bulk state.

Desorption studies help to identify the nature of adsorption and the possibility of recycling the used adsorbent and adsorbate. In such context, the recovery of the adsorbent or, adsorbate is very important (Sathishkumar et al., 2009 and Ansari & Mosayebzadeh, 2011). Generally, a suitable adsorbent for dyes adsorption should meet several requirements: efficient for removal of a wide variety of dyes; (ii) high capacity and rate of adsorption; (iii) high selectivity for different concentrations; (iv) tolerant of a wide range of wastewater parameters; (v) have high regeneration efficiency and also cost effective (Crini, 2006). The fundamental concept in adsorption science is that named as the adsorption isotherm. It is the equilibrium relation between the quantity of the adsorbed material and the pressure or concentration in the bulk fluid phase at constant temperature. Practical application of adsorption processes is based mainly on selective uptake of individual components from their mixtures by other substances (Dabrowski, 2001).

1.4.1 Adsorption isotherms

In order to determine the maximum adsorption capacity (mg g^{-1}), type and mechanism of adsorption, two main isotherm models namely Langmuir and Freundlich are used to describe the adsorption of MO dye. On one hand, the Langmuir isotherm model is based on the assumption of a monolayer adsorption, where all the sorption sites are identical and energetically equivalent (Nawi et al.,

2010). The linearized Langmuir isotherm can be expressed by the equation 1.2:

$$\frac{C_e}{q_e} = \frac{1}{K_L} + \frac{a_L}{K_L} C_e \quad (1.2)$$

Where C_e is the concentration of MO at equilibrium in the liquid phase (mg L^{-1}), q_e is the adsorption capacity at equilibrium (mg g^{-1}), K_L and a_L is the Langmuir isotherm constant in L g^{-1} and L mg^{-1}, respectively. K_L and a_L can be calculated from the intercept and slope of plot C_e/q_e versus C_e. The maximum adsorption capacity of PANI/glass q_{max} is numerically equal to K_L/a_L. On the other hand, the Freundlich isotherm explains the adsorption on a heterogeneous surface with uniform energy and there are interactions between the adsorbed molecules. This means that it is not restricted to the formation of a monolayer (Lunhong et al., 2010). The linearized Freundlich isotherm can be described according to equation 1.3:

$$\ln q_e = \ln K_F + \frac{1}{n_F} \ln C_e \quad (1.3)$$

Where q_e is the adsorption capacity at equilibrium (mg g^{-1}), C_e is the MO concentration at equilibrium in the liquid phase (mg L^{-1}), K_F and n_F is the Freundlich constant related to the bonding energy (L g^{-1}) and adsorption intensity or surface heterogeneity, respectively. K_F and n_F can be calculated from the intercept and slope of plot ln q_e versus ln C_e.

1.4.2 Adsorption kinetics study

In order to investigate the controlling mechanism of the adsorption processes of MO dye, the pseudo-first order, pseudo- second order, intraparticle diffusion and Elovich models were employed to describe the adsorption of MO dye by PANI powder and PANI/glass. The respective equations for pseudo-first order (Abramian & El-Rassy, 2009), pseudo-second order (Cestari et al., 2004), intraparticle diffusion

(Dogan et al., 2009) and Elovich models (Lunhong et al., 2010) are shown in equations 1.4 to 1.7:

$$ln(q_e - q_t) = ln\, q_e - k_1\, t \quad (1.4)$$

$$\frac{t}{q_t} = \frac{t}{q_e} + \frac{1}{k_2\, q_e^2} \quad (1.5)$$

$$q_t = k_i\, t^{0.5} + C \quad (1.6)$$

$$q_t = b + a\, ln\, t \quad (1.7)$$

Where q_e and q_t are the amounts of dye adsorbed (mg g^{-1}) at equilibrium and at time t (min), and t is the adsorption time (min). For the intraparticle equation 1.6, where k_i is the intraparticle diffusion rate constant in mol g^{-1} $min^{-0.5}$ and C is an intercept (mol g^{-1}) proportional to the boundary layer thickness (Ivanov et al., 2003). The other parameters are different kinetics constants that can be determined by the slope of the experimental data.

1.4.3 Thermodynamic study

The effect of temperature on the adsorption of MO dye by the PANI/glass and PANI powder were investigated by varying the temperature from 300-340 K using a water bath. Thermodynamic parameters, such as, Gibb's free energy (ΔG°), the entropy (ΔS°) and the enthalpy (ΔH°) were investigated and calculated using the following relations as shown in equations 1.8 to 1.10:

$$K_c = \frac{C_{Ae}}{C_e} \quad (1.8)$$

$$\Delta G^\circ = -RT\, In\, K_C \quad (1.9)$$

$$\log K_c = -\frac{\Delta S^\circ}{2.303\mathrm{R}} + \frac{\Delta H^\circ}{2.303\mathrm{R}T} \quad (1.10)$$

Where, K_c is the equilibrium constant, C_{Ae} is the amount of dye adsorbed on solid at equilibrium (mg L^{-1}), C_e is the equilibrium concentration of dye in the

solution (mg L^{-1}), R is the gas constant (8.314 J mol^{-1} K^{-1}) and T is the temperature in Kelvin (Nawi et al., 2010). From the the van't Hoff plots of ln K_c versus 1/T the values of ΔH° and ΔS° can be calculated from the slope and intercept.

1.5 Titanium dioxide (TiO_2)

1.5.1 Historical Background

TiO_2 powders have been commonly used as white pigments from ancient times. In the early 20th century, photoactivity of TiO_2 has been reported (Carp et al., 2004). For instance, in 1938 the photobleaching of dyes by TiO_2 both in vacuum and in oxygen have been reported whereby UV absorption produces active oxygen species on the TiO_2 surface, causing the photobleaching of dyes (Hashimoto et al., 2007). It was also known that TiO_2 itself did not change through the photoreaction. In 1956 Kato and Mashio had dispersed TiO_2 powders into various organic solvents such as alcohols and hydrocarbons followed by the UV irradiation with a Hg lamp. They observed the autoxidation of solvents and the simultaneous formation of H_2O_2 under ambient conditions and concluded that the anatase activity of the autoxidation was much higher than that of rutile (Hashimoto et al., 2007). In 1969, the possibility of solar photoelectrolysis was demonstrated for the first time when the system was exposed to near-UV light, and connected to a platinum black counter electrode through an electrical load (Fujishima et al., 2000 and Hashimoto et al., 2007). Fujishima & Honda (1972) had demonstrated the potential of titanium dioxide TiO_2 semiconductor materials to split water into hydrogen and oxygen in a photo-electrochemical cell. Their work triggered the development of a semiconductor photocatalysis for a wide range of environmental and energy applications. Frank & Bard (1977) had reported for the first time the use of titanium dioxide

photocatalysis for the remediation of environmental pollutants in the reduction of CN-8 in water. Use of nano titanium dioxide in an efficient dye sensitized solar cell (DSSC) was reported by O'Regan and Grätzel (1991). Up to now TiO_2 nanoparticles have been applied in purification of pollutants, photocatalytic water splitting, photocatalytic anti bacteria, photo-induced super hydrophilicity as well as in photovoltaics and photosynthesis (Lan et al., 2013).

1.5.2 TiO_2 Structure and Properties

Titanium dioxide (TiO_2) exists in three different polymorphs; anatase, rutile and brookite. In all three forms, titanium (Ti^{4+}) atoms are coordinated to six oxygen (O_2^-) atoms, forming TiO_6 octahedral (Pelaez et al., 2012). The difference between the two crystal structures is the distortion of each octahedral and the assembly pattern of the octahedral chains. Figure 1.2 shows the crystal structure of anatase, rutile and brookite. Anatase is made up of corner (vertices) sharing octahedral which form (001) planes (Figure 1.2a) resulting in a tetragonal structure. In rutile, the octahedral share edges at (001) planes to give a tetragonal structure (Figure 1.2b), and in brookite, both edges and corners are shared to give an orthorhombic structure (Figure 1.2c). The bands gap of anatase, rutile and brokite are 3.2 eV, 3.0 and 3.2 eV respectively (Chatterjee & Mahata, 2004). However, the TiO_2 anatase is more effective in the photocatalytic degradation processes than the TiO_2 rutile. This is attributed to a higher density of localised states and consequent surface-adsorbed hydroxyl radicals and slower charge carrier recombination in anatase relative to rutile (Hanaor & Sorrell, 2011). These different forms of TiO_2 lead to a significant discrepancy in many physical properties as shown in Table 1.3 (Gupta & Tripathi, 2011).

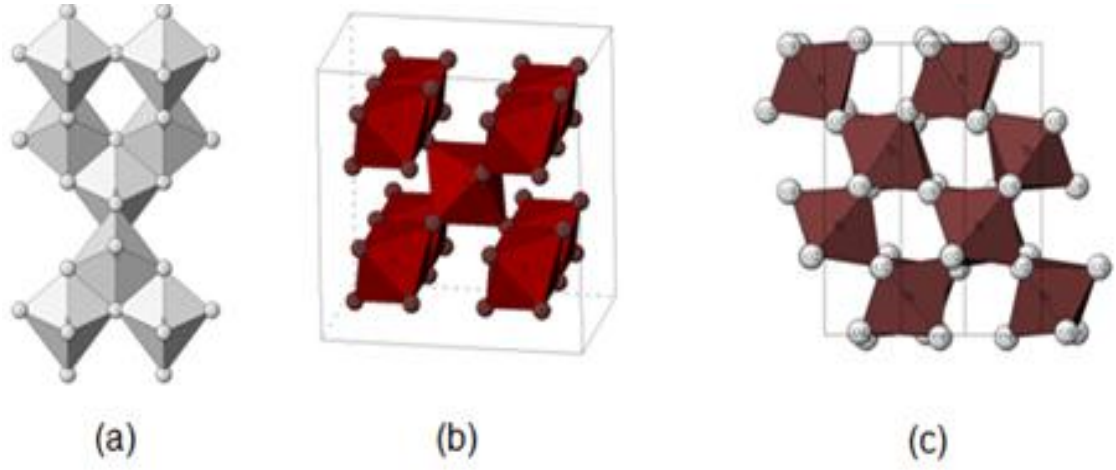

Figure 1.2: Bulk crystalline structures of the (a) anatase, (b) rutile, (c) brookite type TiO_2 (Pelaez et al., 2012).

Table1.3: Summarized the key properties of anatase, rutile and brookite (Gupta & Tripathi, 2011).

Properties	**Rutile**	**Anatase**	**Brookite**
Crystal structure	Tetragonal	Tetragonal	Orthorhombic
Lattice constant (Å)	a = 4.5936	a = 3.784	a = 9.184
	c =2.9587	c = 9.515	b = 5.447
			c = 5.154
Molecule (cell)	2	2	4
Volume/ molecule ($Å^3$)	31.2160	34.061	32.172
Density (g cm^{-3})	4.13	3.79	3.99
Ti–O bond length (Å)	1.949 (4)	1.937(4)	1.87-2.04
	1.980 (2)	1.965(2)	
O-Ti-O bond angle	81.2°	77.7°	77.0°-105°
	90.0°	92.6°	

1.5.3 TiO_2 as a photocatalyst

Among AOPs, photocatalysis using TiO_2 appears as the most emerging effective technology. Many dyes have been successfully degraded in a batch scale by

using both artificial irradiation and solar technology (Damodar & Jagannathan, 2007 and Kodom et al., 2012). Moreover, TiO_2 catalyst is easily available, inexpensive, non-toxic and show chemical inertness (Yao et al., 2010).

The mechanism of photocatalysis involves the ejection of an electron from the valence band to the conduction band of the TiO_2 semiconductor when it is excited with ultraviolet light. At this point, the energy of irradiation used is equal or more than the band gap of anatase TiO_2 (3.2 eV) (Nero et al., 2005). The photoexcitation promotes an electron (e^-) from the valence band and leaves an electronic vacancy or hole (h^+) in the valence band as shown in Figure 1.3. Thus the act of photoexcitation generates an electron-hole pair (Xinshu et al., 2011).

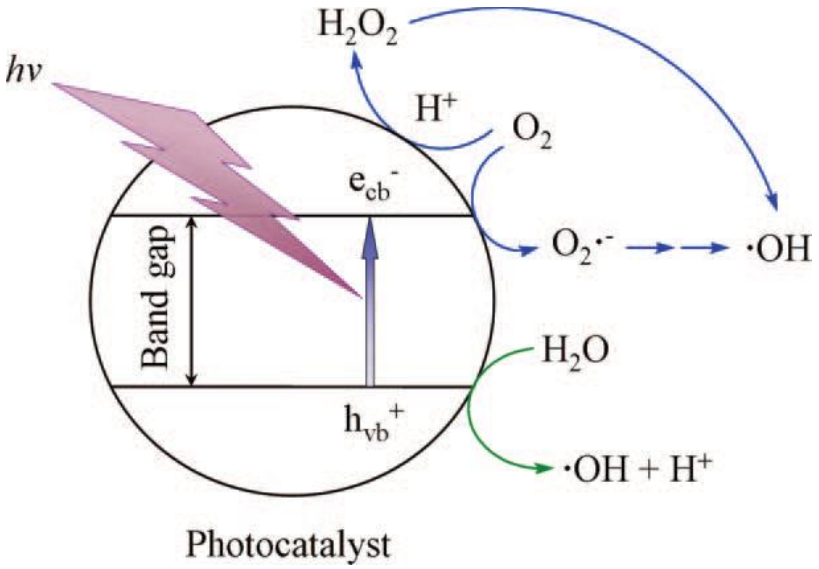

Figure 1.3: Schematic illustration of the photoinduced holes and electron over photon activated semiconductor photocatalyst (Lan et al., 2013).

These species undergo charge transfer reactions across the interface with oxygen, water or organic pollutants on TiO_2 surface. In the valence band, the holes produced by the irradiation migrate to the interface and react with OH^- ions adsorbed onto the TiO_2 to create hydroxyl radicals ($OH^{\cdot}$) which are powerful oxidants to attack the recalcitrant organic compound (R) (Nawi et al., 2012a).

The whole reactions are shown according to equations 1.11 to 1.14:

$$TiO_2 + h\nu \rightarrow h^+ + e^- \quad (1.11)$$

$$h^+ + H_2O \rightarrow OH^{\cdot} + H^+ \quad (1.12)$$

$$OH^{\cdot} + R \rightarrow CO_2 + H_2O \quad (1.13)$$

$$h^+ + R \rightarrow CO_2 + H_2O \quad (1.14)$$

The ejected electrons react with electron acceptors such as oxygen dissolved in water to produce $O_2^{\bullet -}$ leading to the formation perhydroxyl radicals as shown in equations 1.15 and 1.16:

$$e^- + O_2 \rightarrow O_2^{\cdot -} \quad (1.15)$$

$$H^+ + O_2^{\cdot -} \rightarrow HO_2^{\cdot} \quad (1.16)$$

In addition, perhydroxyl radicals will produce hydrogen peroxide as shown in equation 1.17:

$$HO_2^{\cdot} \rightarrow H_2O_2 + O_2 \quad (1.17)$$

Hydrogen peroxide will produce hydroxyl radicals as shown in equation 1.18:

$$H_2O_2 \rightarrow 2OH^{\cdot} \quad (1.18)$$

Without the presence of electron donors or acceptors, the electrons and holes may recombine together to generate heat as shown in equation 1.19:

$$TiO_2(e^-) + TiO_2(h^+) \rightarrow TiO_2 + \text{heat} \quad (1.19)$$

1.5.4 Shortcomings of TiO_2 photocatalyst

Apparently, in degrading hazardous compounds in water effluents, there are obstacles to the viable applications of TiO_2 photocatalysis which are listed as follows:

1. Catalyst reuses: Photocatalytic reactions is usually carried out in slurry modes so that, the need for post treatment or filtration step makes its practical

applications tedious and costly. In addition, the fine TiO_2 particles tend to aggregate especially at high concentrations provides real limitation to apply to continuous flow system and suffer from scattering of incident UV light by the suspended particles.

2. The photocatalytic reactions by TiO_2 is relatively slow because of its low adsorption ability of pollutants which limits its degradation competencies to selective compounds.
3. Recombination of electron and hole may occur either on the surface or in the bulk and is in general facilitated by impurities, defects, or all factors which introduce bulk or surface imperfections into the catalyst.
4. Only a small portion (5 % -7 %) of solar spectrum in the UV region could be absorbed by TiO_2 due to its large band gap energy (3.2 eV) leading to a low degradation rate. Besides that, the use of high-energy UV treatment is expensive and also hazardous to operators.

1.5.5 Strategies for improving TiO_2 photoactivity

Various strategies have been conducted in order to overcome the crucial obstacles mentioned in 1.5.4 and resulted in the improvement in the photocatalytic efficiency of TiO_2. Since practical efficiency of pure TiO_2 for solar application is limited, many modifications have been done to modify the material to facilitate visible light absorption. Among these modifications, doping of TiO_2 with transition metals such as Fe, Co, Cr, and V had been carried out in order to extend the spectral response of TiO_2 into the visible region and improve its photocatalytic efficiency (Han et al., 2004; Reddy et al., 2004 and Pelaez et al., 2012). However, metal

doping has many drawbacks: transition metals may also act as recombination sites for the photo induced charge carriers thus, lowering the quantum efficiency and thermal stability of the system. Deposition of noble metals like Ag, Pt, Au, and Pd on the surface of TiO_2 enhance the photocatalytic efficiency under visible light by acting as an electron trap therefore delaying recombination of the electron-hole pair (Ni et al., 2007; Zaleska, 2008; Liu et al., 2010 and Loganathan et al., 2011). Nevertheless, modification of TiO_2 with noble metals is a limited technology because the process is expensive. Doping TiO_2 with non-metal such as carbon (C), sulphur (S) and particularly nitrogen (N) are the most popular elements being studied by researchers (Wang et al., 2007; Rockafellow et al., 2009; Kusumawardani et al., 2010 and Nawi & Nawawi, 2013) due to its effectiveness in introducing some localized states in the band gap causing the narrowing of the band gap. Different synthesized coupled semiconductors such as ZnO/TiO_2, CdS/TiO_2 and Bi_2S_3/TiO_2 Kanjwal et al. (2011) and Kannaiyan et al. (2010) have been proven to improve the photocatalytic efficiency of TiO_2 by decreasing the recombination rate of the photogenerated electron-hole pairs. The coupling of a large band gap semiconductor with a smaller one had also been proven to activate the system for visible light photocatalysis of organic pollutants using solar radiation (Pelaez et al., 2012). Coating the particles with thin layers of a wide band gap material for blocking the trap states can lead to a drastic enhancement of the photostability (Vogel et al., 1994 and Pelaez et al., 2012). For example, CdS has an ideal band gap energy for solar and visible light applications (2.4 eV). However, CdS is prone to photo anodic corrosion in aqueous environments (Pelaez et al., 2012). When CdS was combined with a wide band gap semiconductor, such as ZnO and TiO_2, it gave improved charge separation

of the photogenerated electrons and holes and improved its photocatalytic activity (Yildiz et al., 2007).

Dye sensitization is another technique being used to improve the photocatalytic activity of TiO_2. The mechanism of the dye sensitized photodegradation of pollutants is based on the absorption of visible light for exciting an electron from the highest occupied molecular orbital (HOMO) to the lowest unoccupied molecular orbital (LUMO) of a dye. The excited dye molecule subsequently transfers electrons into the conduction band of TiO_2, while the dye itself is converted to its cationic radical (Pelaez et al., 2012). Several researchers have reported about the degradation of phenols and its derivatives, surfactants and pesticide by the dye sensitized TiO_2 (Chatterjee & Mahata, 2004; Song et al., 2007 and Dozzi et al., 2013). However, dye sensitized TiO_2 performance is limited as an environmental remediated due to the dye molecule that was only adsorbed on the TiO_2 surface and chemical bonds formed is not stable therefore, the dye molecules was easy to desorb or degrade from TiO_2 surface during the photocatalytic process thus eventually decreases its photocatalytic activity.

Combining TiO_2 with adsorbents would be of great interest. The adsorbent not only offer a support for the TiO_2, but would also provide higher specific surface area and facilitate more effective adsorption than bare TiO_2 due to its ability to concentrate the pollutants and intermediates around the surface of TiO_2 where they would be degraded through combined adsorption-photocatalytic synergistic effect (Carpa et al., 2004 and Zhang et al., 2009). Nowadays, numerous studies have revealed that many adsorbents exhibited a multi-functional performance with TiO_2 in heterogeneous photocatalytic process such as chitosan (Zubieta et al., 2008 and Nawi et al., 2012b) activated carbon (El-Sharkawy et al., 2007), silica (Kirtay et al., 2006)

and polyaniline (PANI). For instance, Olad et al. (2012) had reported that TiO_2/PANI core-shell nanocomposite showed better photocatalytic activity for MO photodegradation compared to the pristine TiO_2 nanoparticles. They have attributed this improvement to reduced aggregation state of TiO_2 nanoparticles in PANI/TiO_2 nanocomposite which led to the higher specific surface area. Therefore, adsorption of dye molecules on the nanocomposite was higher than pristine TiO_2. However, most of the conducted studies have used TiO_2 suspended in aqueous medium which make recycling process troublesome and penetration of UV is limited due to the aggregation of the nanoparticles. To eliminate the need for post-treatment and the problem of agglomeration, immobilization of TiO_2 on solid supports is an alternative and a convenient method for long time applications. TiO_2 may be immobilized on suitable solid supports such as quartz, sand, glass, silica, ceramics, activated carbon, zeolites and stainless. Several techniques have been developed for immobilizing TiO_2 catalysts onto a solid substrate including a sol gel method (Yao et al., 2010 and Xinshu et al., 2011), electrophoretic deposition (EPD) (Nawi et al., 2003 and Kodom et al., 2012) etc. However, the main disadvantage of the EPD is the necessity of a subsequent sintering of the coatings, which may lead to detrimental mechanical properties of the metal or alloy.

Application of sol-gel technique for immobilization of TiO_2 requires the conversion of the hydrolysed titanium into anatase TiO_2 and this process needs a calcination treatment. Furthermore, the fixing of the catalyst on the solid supports would decrease the surface area available for the reaction as well as the porosity of the supported catalyst layer that in turn reduces the photocatalytic efficiencies of the immobilized TiO_2 (Lathasree et al., 2004). Table 1.4 summarized the related works on the modified TiO_2 for the photocatalytic degradation of organic pollutants.

Table1.4: Related works on the modified TiO_2 for the photocatalytic degradation of organic pollutants.

Application	Researches	Study	Findings
Photodegradation of phenol and (MO).	Yao et al. (2010)	• Preparation and immobilization of (TiO_2) on (ACF) by sol-gel method and calcination.	• Immobilized (TiO_2/ACF) was prepared by sol-gel method followed by calcination from 300 to 600 °C. • (TiO_2/ACF) photocatalyst can degrade organic pollutants under UV irradiation particularly the calcined sample at 500 °C. • Kinetics analysis is described by a first-order rate equation. • (TiO_2/ACF) photocatalyst can be recycled and easy recover after the reaction.
Photocatalytic removal of RR4 and MB.	Nawi et al. (2012a) and Nawi & Zain (2012)	• Synthesis a coating solution of TiO_2, epoxidized natural rubber (ENR-50) and (PVC) in a mixture of toluene and CH_2Cl_2. • Photocatalytic efficiency of immobilized TiO_2 onto glass plate.	• Immobilizing TiO_2 powder onto solid supports has been successfully developed using ENR/PVC blend as the adhesives. • Most of the ENR polymer in the TiO_2/ENR/PVC plate was removed by a 45 W compact fluorescent lamp for 5 h

			in ultra-pure water which resulted in an increase in specific surface area, bigger pore volume size, smaller particle size and high mechanical strength. • The immobilized P-25TiO_2/ENR/PVC/5 h catalyst plate showed comparable photocatalytic activity in degrading RR4 and MB to the TiO_2 slurry system. • TiO_2/ENR/PVC/5h catalyst plate was found to be reusable, sustainable with photocatalytic efficiency was better than 99 % after ten runs.
Photocatalytic degradation of Phenol.	Li et al. (2008)	• Preparation PANI-modified TiO_2 composites by 'in situ'chemical oxidative polymerization of aniline in the TiO_2 suspension. • Degradation of phenol to evaluate the photocatalytic activities of the modified catalysts.	• TiO_2 nanoparticles are deposited by PANI which reduce TiO_2 particles agglomeration. • According to the X-ray diffraction the modification does not alter the crystalline structure of the TiO_2 nanoparticles. • UV–vis spectra revealed that PANI-modified TiO_2 composites showed stronger absorption than pristine TiO_2 under the whole range of visible light. • PANI-modified TiO_2 showed significantly higher photocatalytic activity than pristine TiO_2 under visible light. • The PANI-modified TiO_2 particulates have good photo

			stability and photocatalytic activity and can be recycled five times.
Phenol photodegradation.	Tasseroul et al. (2012)	• Introducing nickel (II) tetra (4-carboxyphenyl) porphyrin (TCPPNi) in one step into the TiO_2 matrix by the sol–gel process. • A Kinetic study of p – nitrophenol degradation. • To evaluate the photoactivity of xerogels for p-nitrophenol degradation in aqueous medium at 20 °C.	• The introduction of porphyrin led to a diminution of the specific surface area of TiO_2 xerogels. • Porphyrin doped TiO_2 degraded more than 40 % of the p-nitrophenol while non-doped TiO_2 xerogel degraded only 10 %. Moreover, porphyrin was found to improve the photoactivity of TiO_2 xerogels in a similar way to UV-A pretreatment. • The best kinetic model involved one type of active site corresponding to the hole h+ of electron-hole pairs created at the TiO_2 surface by light.
photodegradation of MO	Lei et al. (2012)	• Preparation hybrid film of (PVA)/TiO_2 via solution-casting combined with heat-treatment method.	• TiO_2 nanoparticles have immobilized in PVA matrix by Ti O C chemical bonds via dehydration reaction between TiO_2 and PVA during the heat treatment process. • The film with 10 wt % TiO_2 and treated at 140 °C for 2 h showed a remarkable ultraviolet (UV) photocatalytic activity for photodegradation of MO approximately close to the TiO_2 slurry system. • The good swelling ability of PVA matrix provided the good contact between MO molecules and TiO_2 which

			benefited the photocatalysis.
Photodegradation of Methyl Orange under UV and visible-light irradiation.	Wang & Zhou (2011)	• Preparation a composite bycoupling CNTs with phosphorus-doped TiO_2 was by hydrothermal method. • To investigate the morphology and the physicochemical properties using TEM, XPS, XRD, BET, FTIR, TG-DSC and UV-VIS DRS spectroscopy.	• It was found that the novel CNTs/P-TiO_2 photocatalyst has smaller crystalline size, larger surface area and stronger absorption in the visible range than pure TiO_2. • The novel CNTs/P-TiO_2 photocatalyst exhibited higher photocatalytic activity than P25 and pure TiO_2 due to the surface states of phosphorus allow the more efficient utilization of both UV and visible-light and the presence of CNTs promotes the separation of photogenerated carriers.
Photocatalytic degradation of Rhodamine and Methylene blue.	Wang et al. (2010)	• Synthesis of PANI/TiO_2 nanocomposite by the oxidative polymerization of aniline with ammonium peroxydisulfate in water without the addition of acid. • Study the morphological, structural and optical properties of PANI/TiO_2.	• TiO_2 anatase crystal structure and a PANI monolayer on surface of the TiO_2 was confirmed by the XRD pattern and TEM measurements. • PANI/TiO_2 nanocomposite showed higher photocatalytic efficacy compared to bare TiO_2.

Combining adsorption and oxidative photocatalytive for removal air pollutant	Matos et al. (2010)	The influence of AC onto activity of TiO_2 in toluene photooxidation.	• TiO_2-AC was more efficient than TiO_2 alone to photooxidation toluene.
Air disinfection photoreactor	Olayr et al. (2013)	• Preparation catalyst by photodeposition of Ag, Pd and Fe on commercial TiO_2 immobilized on glass plate. • Determine the atomic percentage and species onto the TiO_2 surface. • Evaluating the photocatalytic inactivation of three bacteria, E. coli, B. coli, C. coli.	• XRD analysis showed that 85 % of silver, 73 % of Pd and 45 % of Fe were present in metallic form on TiO_2 surface. Inactivation (50 %) of E. coli while 41 % and 35 % inactivation of B. subtilis and S. aureus were obtained, respectively by bare TiO_2 photocatalyst coated glass. • Inactivation with Pd-TiO_2 achieved more than 90 % B. subtilis and S. aureus with a very short residence time of 14s inactivation of E. coli was not significantly increased when metal modified TiO_2 was used, ranging from 47 % to 57 %.
Disinfection	Kubacka et al. (2008)	• Adding Ag into TiO_2 by impregnation and photodeposition methods. • Analysis the anti-microbial properties of catalyst as a function of the silver content using E. coli.	• Silver content around 1 wt. % maximizes the photokilling activity. • Silver would help increasing adhesion of bacteria to the titanium surface.

Water splitting technology and photocatalytic degradation of MB.	Babu et al. (2012)	• Preparation nitrogen doped TiO_2 (N-TiO_2) using sol gel, electrospining and post-annealing of the composite nano fibers. • Photodegradation of MB under visible light. • Utilizing N-TiO_2 for water splitting and evaluating hydrogen (H_2).	• The first order rate constant for degradation of MB were found to be highest for N-TiO_2. • N-TiO_2 has improved surface area and enhanced hydrogen production and efficiency.

1.6 Polyaniline (PANI) conducting polymer

Conductive polymers or "organic metals" are materials made from organic building blocks (Atassi et al., 2008). It has the electronic properties of semiconductors and mechanical parameters of polymers (Anand et al., 1998 and Bhattacharya & Misra, 2004). Conducting polymers are characterized by a conjugated structure of alternating single and double bonds. The feature shared by all of them originates from the common nature of their π-electron system, an enhanced conductivity in oxidized or in reduced state and reversible redox activation in a suitable environment (Atassi et al., 2008). Among these polymers, PANI is found to be the most promising due to its unique electrical, electrochemical properties, high environmental stability, easy of synthesis, tuneable properties and low cost of monomer (Bhadra et al., 2009; Choudhury, 2009 and Ansari & Mosayebzadeh, 2011). PANI can be synthesized by the oxidative polymerization of aniline in acidic media using variety of oxidizing agent such as $(NH)_4S_2O_8$, KIO_3 and $K_2Cr_2O_7$ (Ansari & Keivani, 2006 and Ansari & Mosayebzadeh, 2011) or electrochemically in aqueous and non-aqueous solvents (Ansari & Mosayebzadeh, 2011 and Ayad et al., 2013). PANI could be found in one of three idealized oxidation state: Leucoemraldine (white), Emeraldine (green) and Pernigraniline (blue/violet). However, Emeraldine salt is the only conductive form while the other have poor conduction. PANI is consisted of two types of benzenoid (reduced) and quinonoid (oxidized) units when Pernigraniline form is fully reduced and permiglaniline form is fully oxidized (Laslau et al., 2010). Figure 1.4 shows the possibility of PANI to convert from the PANI base to PANI (emeraldine salt) after the protonation in the acidic conditions (Ayad et al., 2013).